Title: Characterization and Evaluation of a Mass Efficient Heat Storage Device.

Authors:

Scott C. Splinter, Max L. Blosser,
NASA Langley Research Center, Hampton, VA

Andrew R. Gifford,
Virginia Polytechnic Institute and State University, Blacksburg, VA

ABSTRACT

The heat sponge is a device for mass-efficient storage of heat. It was developed to be incorporated in the substructure of a reentry or hypersonic vehicle to reduce thermal protection system requirements. The heat sponge consists of a liquid-vapor mixture contained within a number of miniature pressure vessels that can be embedded within a variety of different types of structures. As temperature is increased, pressure in the miniature pressure vessels also increases so that heat absorbed through vaporization of the liquid is spread over a relatively large temperature range. Using water as a working fluid, the heat storage capacity of the liquid-vapor mixture is many times higher than that of typical structural materials and is well above that of common phase change materials over the temperature range of 660^{o}R to 1160^{o}R. Prototype heat sponges were fabricated and characterized. These heat sponges consisted of 1.0 inch diameter hollow stainless steel spheres with a wall thickness of 0.020 inches which had varying percentages of their interior volumes filled with water. An apparatus to measure the heat stored in these prototype heat sponges was designed, fabricated, and verified. The heat storage capacity calculated from measured temperature histories is compared to numerical predictions.

INTRODUCTION

Hypersonic vehicles experience extreme aero-thermodynamic heating which requires the use of Thermal Protection Systems (TPS) to survive and regulate the

Scott C. Splinter and Max L. Blosser, NASA Langley Research Center, Structural Mechanics and Concepts Branch, 8 West Taylor Street, MS 190, Hampton, VA 23681
Andrew R. Gifford, Virginia Polytechnic Institute and State University, Blacksburg, VA 24061 (Doctorate Student)

heat transfer to and from the vehicle in order to maintain structural integrity. Detailed studies of the thermal performance of insulating TPS concepts by Myers et al. [1] and Blosser [2] found that the heat capacity of the vehicle structure is one of the most influential factors determining TPS thermal performance. An increase in heat capacity of the vehicle structure would allow it to absorb more of the incident heat load without exceeding its structural temperature limit. Therefore a thinner, lighter insulator could be applied because it does not have to inhibit as much of the incident heat load [1]. Previous design processes focused on optimizing the weight of the insulation material and sizing it to limit the temperature of whatever structure was selected by the structural designers. Options for enhancing the specific heat capacity of the vehicle structure have been investigated by Blosser [3], leading to the concept of a mass-efficient, heat-storage device called the heat sponge.

A number of structural and non-structural materials were investigated by Blosser [2, 3] as candidates for enhancing the heat capacity of structures. Beryllium and Lithium were identified as two materials that had high heat storage capacities, but also had many hazards and drawbacks associated with their use. Liquids were also investigated by Blosser [3] for use as a thermal storage medium, with water having the most attractive properties out of the candidates. However, water is usually not considered for high temperature applications because it boils at 672^{o}R. By encapsulating the water in a pressure vessel, or series of miniature pressure vessels, it can be used to store heat at temperatures beyond its boiling point. A further benefit of encapsulation is that it takes advantage of water's high latent heat of vaporization to store additional amounts of heat energy. Blosser developed the concept of the heat sponge to contain a liquid-vapor mixture of water within a pressure vessel, or a number of miniature pressure vessels, for the purpose of efficiently absorbing heat [3]. Figure 1 shows a sketch of a generic pressure vessel containing a liquid-vapor water mixture. Different effective heat capacities can be obtained by varying the initial interior volume percentage of water. This allows the heat sponge to be optimized to achieve different efficiencies per unit mass or volume. Figure 2 shows the different specific heat capacities of a liquid-vapor water mixture, excluding the container, with the specific heat capacity of Lithium.

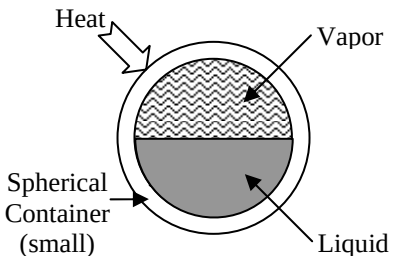

Figure 1. Heat sponge concept

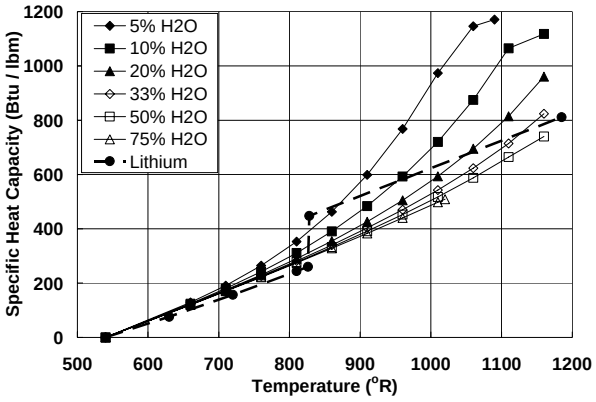

Figure 2. Preliminary heat capacities of liquid-vapor water mixture

Another important factor that must be considered is containing the pressure generated by the constant volume phase change of water. While these pressures can be manageable for most pressure vessels, the energy contained in the vessels will not be large due to the small size and nature of the vessels, so that the failure of a single pressure vessel may not be catastrophic [3].

PROTOTYPES

Heat sponge prototypes were developed to assess the feasibility of the concept. The prototypes needed to be large enough to be easily filled, instrumented, and handled, yet small enough to limit the stored energy and influence of the container on the overall effective specific heat capacity. Hollow, spherical specimens, 1 inch in diameter, were selected as test articles that could be readily fabricated and tested. Spherical geometry was chosen for its simplicity and efficiency at containing the high pressures. Stainless steel type 304 was selected as the sphere material for its strength, resistance to corrosion, and customary use in metal spinning fabrication, a process by which metal sheets are spun and bent to form hemispherical shapes. These hemispheres were then laser welded together, to produce the 1 inch diameter hollow spheres. The wall thickness of the prototype spheres were estimated by using the yield strength of 38 ksi for 304 stainless steel, the critical pressure of 3204 psi for water, and the 1 inch constraint on the diameter of the sphere. Calculations were performed using the equation for stress in a spherical pressure vessel to produce an acceptable 0.020 inch wall thickness [4].

Each hollow sphere was converted into a heat sponge test article by the following process. First, a small hole was drilled through the wall of the sphere to allow the needle of a syringe to pass through. Then a predetermined mass of water, based on the initial percentage of the interior volume to be filled and the density of water at 530^{o}R, was injected into the hollow sphere with the syringe. Initial interior volumetric percents of 5%, 10%, 25%, 33%, 40%, 50%, and 60% water were chosen. Two different methods of sealing the hole for the syringe were tried for these experiments. The first method used an epoxy patch, and the second, more preferred method used a silver solder patch. Figure 3 shows the progression of the heat sponge prototypes from a hemisphere, to a sphere, to an instrumented sphere with an epoxy patch. More details can be found in Reference 5.

Figure 3. Heat sponge prototypes

EXPERIMENTAL APPROACH

The primary limitations in using available heat capacity characterization methods for characterizing the heat sponge prototype test article were its physical properties; its size, shape, and mass, coupled with its internal liquid-vapor phase change. Therefore a hybrid technique and a new apparatus were designed for the characterization of the heat sponge test article's heat capacity. The 1 inch diameter spherical test article was uniformly heated to a temperature of 880^{o}R in a 1.5 inch diameter, 6 inch long cylindrically coiled cable heater. Temperature of the cable heater was monitored by three Type-K thermocouples located at the top, middle, and bottom of the cylinder. Temperature of the spherical test article was monitored by six Type-T thermocouples, five were spaced along a longitudinal line and the sixth was located at the equator along a longitudinal line 180 degrees from the first. A strain gage was installed on the same longitudinal line as the sixth thermocouple to determine interior pressure from the strain on the test article. The test article was transferred from the heating chamber to the cooling chamber in approximately 5 seconds by a stepper motor. The test article was cooled back to room temperature in the cooling chamber which consisted of an 8 inch length of straight 2 inch diameter copper pipe wrapped by 3/8 inch diameter copper tubing. The temperature in the copper pipe was monitored by four Type-K thermocouples spaced evenly around the middle of the pipe, and was maintained by a recirculation chiller via the tubing at temperatures less than or equal to 520^{o}R. The apparatus is shown in Figure 4. The temperatures recorded during the cool down of the test article were used to determine its temperature dependent specific heat capacity.

The most difficult challenge in implementing this approach was to effectively characterize the heat lost from the test article as it cooled. This task was simplified by designing the apparatus to eliminate or minimize all heat transfer modes except one, radiation. The apparatus was enclosed by a vacuum chamber at a pressure below 2x10^{-4} torr to minimize convection and gas conduction. The test article was

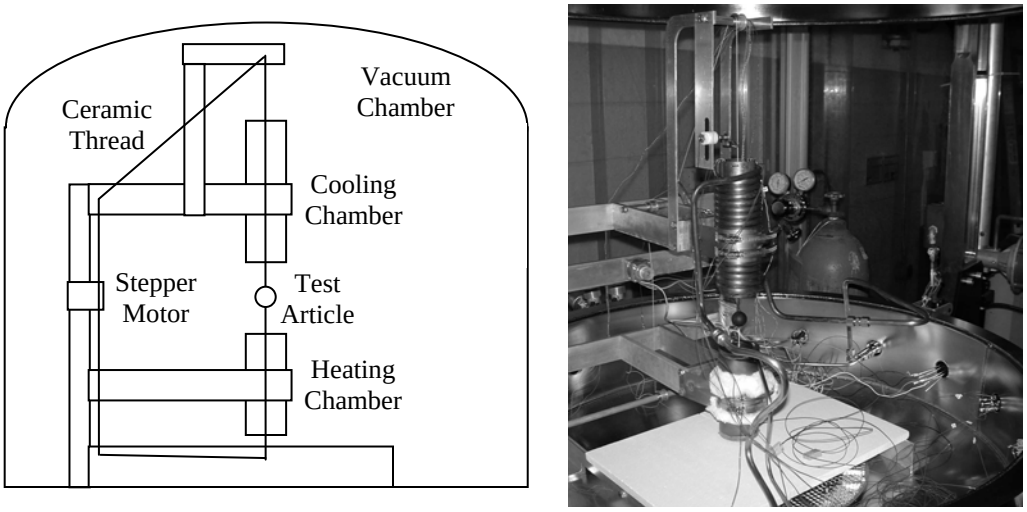

Figure 4. Heat sponge heat capacity characterization apparatus

suspended with low-conductivity ceramic thread to minimize solid conduction. The surfaces of the test article and cylindrical chambers were painted with a high temperature optical black coating with an emissivity/absorptivity of 0.92 across the wavelengths of 0.5 μm to 20 μm. The dimensions of both cylindrical chambers provided a view factor of 0.97 or better from the test article to each chamber. More details can be found in Reference 5.

ANALYTICAL APPROACH

Heat Transfer Model

Analytical models were developed both to predict and to evaluate the performance of the heat sponge concept. Since the test environment was reduced to radiation heat transfer, and the optical black coatings had an emissivity/absorptivity of 0.92 over a majority of the peak infrared wavelengths, the test articles and chambers were assumed to be gray bodies. The net rate of radiation transfer in an enclosure consisting of any two gray surfaces, where the enclosed gray surface does not radiate back on itself, can be represented by [6]:

$$q_{i-j} = F_{i-j}\sigma\left(T_i^4 - T_j^4\right) \tag{1}$$

where $F_{i\text{-}j}$ is an effective factor that combines the shape factor and emissivity for the system, σ is the Stefan-Boltzmann radiation constant, T_i is the test article temperature, and T_j is the constant temperature of the cooling chamber.

Equation (1) is valid only if the cylinder is considered to be a single surface, because the enclosed spherical surface does not radiate back on itself [6]. However, the cylindrical chamber in this case has two holes at each end which act like black bodies at temperatures different from the cylinder wall. Instead of performing a more complex net radiation transfer analysis for a sphere enclosed by a multi-surface concentric cylinder, it was decided and shown in Reference 5, that Equation (1) was a good approximation of the net radiation exchanged for these experiments. The term $F_{i\text{-}j}$ was quantified experimentally as an effective factor for the system through the calibration of the apparatus to a solid aluminum 2024 sphere, which is discussed later in this article.

The conservation of energy principle for a control volume then provides the governing equation for this experimental analysis. The test article does not generate its own energy and any incident energy or spatial temperature variations are assumed to be negligible. The volume and surface area integrals relating to the energy stored and leaving the system are then integrated to produce [7]:

$$\rho\, Cp\, \frac{dT_i}{dt} V + F_{i-j}\sigma\left(T_i^4 - T_j^4\right) A = 0 \tag{2}$$

where ρ is the density of the test article, Cp is the specific heat capacity of the test article, V is the volume of the test article, A is the surface area of the test article, and

dT_i/dt is the derivative of the test article temperature with respect to time. Equation (2) was used for two different purposes; the first was to predict the temperature history of the test article using an estimated specific heat capacity and a fourth order Runge-Kutta scheme [8], and the second was to evaluate the experimental effective specific heat capacity of the test article from measured quantities. No temperature predictions will be presented in this article.

To evaluate the experimental effective specific heat capacity of the test articles, Equation (2) was solved for *Cp*. The temperature derivative was approximated by using a first order centered finite-difference formula with respect to time [8]. The experimental effective specific heat capacity was then calculated by substituting in the average measured test article and cooling chamber temperatures for T_i and T_j respectively. For comparison with the experimental data, high order polynomial functions were fitted to table and chart data for the specific heat capacity of each material versus temperature [9,10]. The specific heat capacity versus temperature data for water pertaining to its phase change was generated by a numerical thermodynamic model which will be explained later in this article. The specific heat capacity of the liquid-vapor water mixture was mass averaged together with the specific heat capacity of the stainless steel container to produce an effective specific heat capacity for the heat sponge. More details can be found in Reference 5.

Thermodynamic Model

A numerical thermodynamic model was developed to calculate the specific heat capacity of water as it transitioned through its phase change at a constant volume and mass. The heat sponge was modeled as a closed thermodynamic system because the liquid-vapor water system was completely enclosed by the stainless steel sphere. A simplified model neglecting air within the heat sponge sphere is shown in Figure 5. This model assumed that the sphere contained a given initial

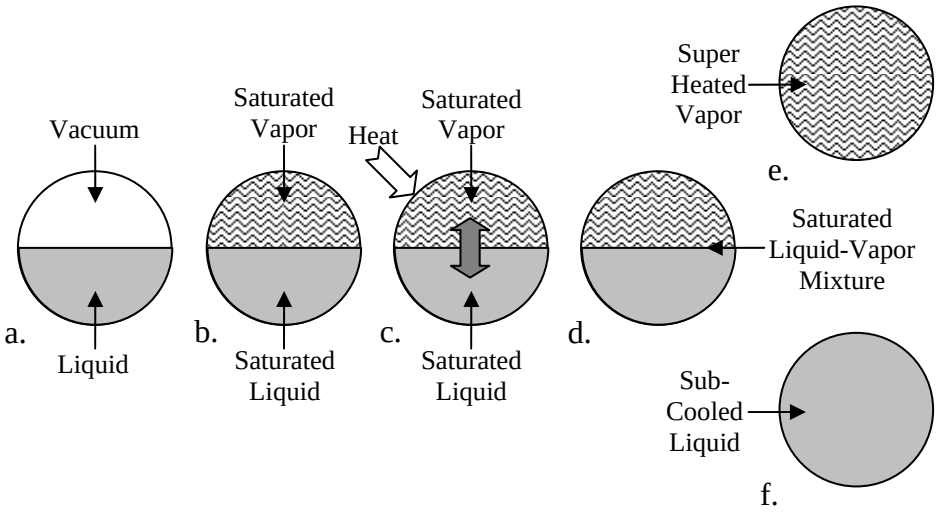

Figure 5. Ideal thermodynamic model of heat sponge

interior volume percentage and mass of liquid water at room temperature in non-equilibrium contact with vacuum which occupied the remaining interior volume of the sphere as shown in Figure 5a. This closed system reaches equilibrium through the evaporation of the liquid water into water vapor until the saturation pressure of water has been reached at room temperature. This room temperature, saturated equilibrium state is called a closed saturated system, as shown in Figure 5b, and provides the initial conditions for the heat sponge thermodynamics model. This system must follow two imposed physical constraints on its mass and volume. The first physical constraint is that the total number of moles of water in the system remains constant, and the second physical constraint is that the total volume occupied by the two phases of water equals the internal volume of the sphere. An increase in the temperature of the system from room temperature by the addition of heat causes water molecules to transfer between liquid and vapor, as shown in Figure 5c, changing the volume and mass of the liquid water and water vapor. The changes in the liquid and vapor volumes are calculated by first linearly interpolating in the steam tables for the saturated specific volume properties of water at the new system temperature [11,12]. Then these saturated specific volume properties are subjected to the physical constraints of the system to determine the new liquid and vapor volumes, and consequently the new liquid and vapor masses. Knowing the new liquid and vapor volumes and masses, the vapor volume fraction and quality of the system can be calculated for the new saturated equilibrium state corresponding to the new temperature. The saturated specific internal energy and enthalpy of the liquid and vapor components of the system are determined in the same manner as the saturated specific volume was, by interpolating in the steam tables with the new saturated system temperature. The interpolated saturated specific internal energies and enthalpies of the liquid water and water vapor are each combined using the quality of the system to determine the specific internal energy and specific enthalpy of the new saturated equilibrium state. This process continues until the system reaches at or before the critical temperature of water, 1165^{o}R, one of three final states. The first state is a two-phase saturated mixture, as shown in Figure 5d, for initial interior volume percentages of water between 20% and 50%. The second state is a superheated vapor, as shown in Figure 5e, for initial interior volume percentages of water between 1% and 20%. Finally, the third state is a sub-cooled liquid, as shown in Figure 5f, for initial interior volume percentages between 50% and 99%. The specific heat capacity for the given initial interior volume percentage and mass of liquid water is then found by calculating the change in the specific enthalpy versus temperature. More details can be found in Reference 5.

EXPERIMENTS

Aluminum Calibration Experiments

The specific heat capacity of a 1.0 inch diameter solid aluminum 2024 sphere was characterized first using this new method and apparatus in order to calibrate the equipment and validate the method. The solid aluminum sphere had a mass of 0.05273 lb_m (23.92 g). Aluminum 2024 was chosen because it has a high specific

heat capacity for a structural material, and is inexpensive and readily available. Specific heat capacity values versus temperature for aluminum 2024 were taken from a handbook [10] and fitted with a polynomial to be used as a calibration reference. Handbook values and the polynomial were assumed to be accurate and without error. Four series of tests were performed by Splinter [5] and Gifford [13] with this calibration sphere for temperatures between 860°R and 500°R, and after multiple improvements to the apparatus and method, a value for F_{i-j} of 0.916 was established. Results are presented in Figure 6 and Table I. Figure 6 is a graphical display of the experimental values overlaid with the handbook values with bands denoting the uncertainty in the experimental measurement. Table I displays the average Cp value, average RMS deviation of experimental value from handbook value, and the average uncertainty in the experimental measurement for the aluminum sphere at each of the listed temperatures.

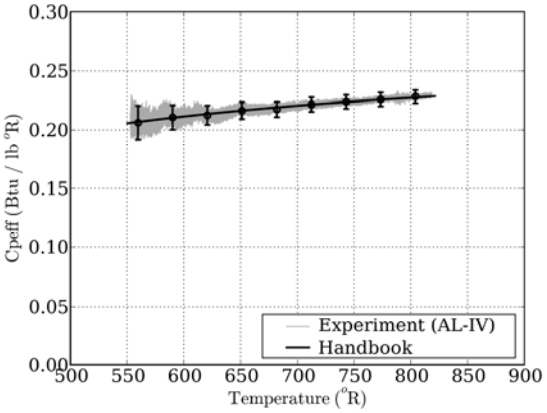

Figure 6. AL 2024 Cp results

TABLE I. AL Cp RESULTS

Temp. (°R)	Cp (Btu / lb°R)	RMS Dev. (Btu / lb°R)	Uncertainty (Btu / lb°R)
804.01	0.2284	0.0009	0.0056
773.44	0.2260	0.0006	0.0058
743.00	0.2239	0.0009	0.0059
712.33	0.2216	0.0010	0.0062
681.85	0.2174	0.0021	0.0064
651.17	0.2164	0.0017	0.0071
620.65	0.2126	0.0024	0.0082
590.12	0.2107	0.0032	0.0102
559.65	0.2062	0.0054	0.0143

Water-Filled Heat Sponge Experiments

Experimental specific heat capacity results were obtained using the validated method and equipment for 10%, 20%, 33%, and 60% water-filled, stainless-steel, heat-sponge test articles, and were compared to their respective numerical predictions generated by the theoretical models. The 10%, 33%, and 60% water-filled test articles were chosen because they transition to one of the final equilibrium states of the heat sponge concept; superheated vapor, saturated mixture, and sub-cooled liquid respectively [5]. The 20% and a second 33% water-filled test article were chosen for additional concept characterization and comparison purposes respectively, after the multiple improvements had been made to the apparatus and method. The results for the second 33% water-filled test article are presented in Figure 7 and Table II, which are similar to Figure 6 and Table I.

The second 33% water-filled test article had a mass of 0.02200 lb_m (9.98 g). When comparing the mass and specific heat capacity of the 33% water-filled test article to the aluminum calibration sphere at a temperature near 775°R, the 33% water-filled test article had more than one and a half times, 165%, the specific heat

capacity of the aluminum calibration test article with less than half, 42%, of its mass. Though quantitative results for the 10% water-filled test article are not shown here, its specific heat capacity was equivalent to the aluminum calibration sphere near 775°R, however it had only 36% of its mass. Similarly for the 60% water-filled test article, its specific heat capacity near 775°R was two times, 208%, that of the aluminum calibration sphere with almost exactly half, 49%, of its mass. Figure 8 displays the results for the 10%, 20%, 33%, and 60% water-filled, heat sponge, test articles. The upward sloping trend and increased noise in the lower temperature region of the experimental results were caused by strain gauge heating and the small temperature delta between the test article and cooling chamber, respectively. These effects were reduced in the 20% and second 33% water-filled test articles by improvements made to the apparatus and method [13]. These experiments show that by containing the liquid-vapor phase change of water inside a spherical pressure vessel, the effective specific heat capacity of the vessel can be raised significantly.

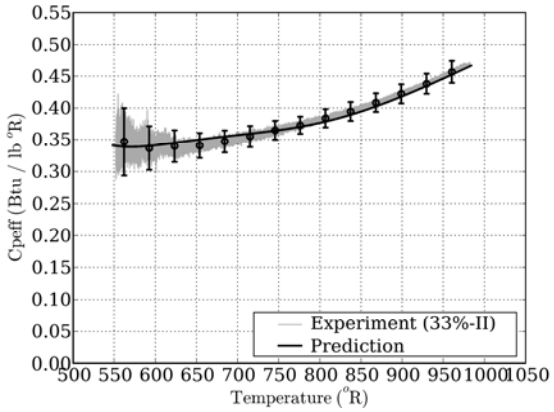

Figure 7. 33%-II water-filled Cp results

TABLE II. 33%-II Cp RESULTS

Temp (°R)	Cp (Btu / lb°R)	RMS Dev. (Btu / lb°R)	Uncertainty (Btu / lb°R)
960.21	0.4570	0.0049	0.0173
929.41	0.4382	0.0039	0.0158
898.86	0.4224	0.0049	0.0151
868.10	0.4085	0.0064	0.0147
837.31	0.3947	0.0060	0.0148
806.71	0.3838	0.0057	0.0144
776.05	0.3728	0.0035	0.0137
745.53	0.3648	0.0023	0.0148
714.90	0.3550	0.0051	0.0164
684.39	0.474	0.0081	0.0171
653.74	0.3409	0.0098	0.0194
623.25	0.3401	0.0072	0.0248
592.68	0.3369	0.0096	0.0341
562.20	0.3470	0.0195	0.0529

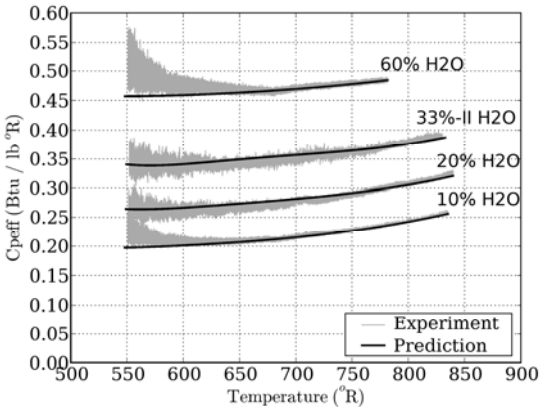

Figure 8. 10%, 20%, 33%, & 60% water-filled heat sponge Cp results

CONCLUSIONS

The prototype heat sponge test articles successfully validated the potential of the heat sponge concept. These experiments showed that by containing the liquid-vapor phase change of water inside a spherical pressure vessel, the effective specific heat capacity of the vessel was raised significantly. Verification of this can be found in the comparison of the 33% water-filled, heat sponge test article with the aluminum calibration test article. The 33% water-filled, heat sponge test article had more than one and a half times, 165%, the specific heat capacity of the aluminum calibration test article while having less than half, 42%, of its mass near 775^{o}R. Therefore, the heat sponge concept is an attractive candidate for further studies of efficient heat storage. The analytical models and techniques developed in this investigation can contribute significantly to these future efforts.

REFERENCES

1. Myers, D. E.; Martin, C. J.; and Blosser, M. L.: "Parametric Weight Comparison of Advanced Metallic, Ceramic Tile, and Ceramic Blanket Thermal Protection Systems," NASA TM-2000-210289, June 2000.
2. Blosser, M. L.: "Advanced Metallic Thermal Protection Systems for Reusable Launch Vehicles," Ph.D. Dissertation, Dept. of Mechanical and Aerospace Engineering, Univ. of Virginia, Charlottesville, VA, May 2000.
3. Blosser, M. L.: "Heat Sponge – Mass-Efficient Thermal Storage for Multifunctional Structures" LAR CASE No. 16282-1, Date 3/6/2001. LaRC Invention Disclosure.
4. Beer, F. P., and Johnston, E. R. Jr., *Mechanics of Materials*; 2nd Ed., 1992, McGraw-Hill, New York, NY
5. Splinter, S. C.: "Characterization and Evaluation of a Mass Efficient Heat Storage Device," Master's Thesis, Dept. of Mechanical and Aerospace Engineering, The George Washington University, Washington D.C., August 2004.
6. Kreith, F., and Bohn, M. S., *Principles of Heat Transfer*; 6th Ed., 2001, Brooks/Cole, Pacific Grove, CA
7. Incropera, F. P., and DeWitt, D. P., *Fundamentals of Heat and Mass Transfer*; 4th Ed., 1996, John Wiley & Sons, New York, NY
8. Chapra, S. C., and Canale, R. P., *Numerical Methods for Engineers*; 3rd Ed., 1998, McGraw-Hill, New York, NY
9. Brown, W. F. Jr., Mindlin, H., and Ho, C. Y., *Department of Defense; Aerospace Structural Metals Handbook* Vol. 2, 1994, Purdue Research Foundation, West Lafayette, IN
10. Brown, W. F. Jr., Mindlin, H., and Ho, C. Y., *Department of Defense; Aerospace Structural Metals Handbook* Vol. 3, 1994, Purdue Research Foundation, West Lafayette, IN
11. Moran, M. J. and Shapiro, H. N., *Fundamentals of Engineering Thermodynamics*; 4th Ed., 2000, John Wiley & Sons, New York, NY
12. Keenan, J. H., Keyes, F. G., Hill, P. G., and Moore, J. G., *Steam Tables; Thermodynamic Properties of Water Including Vapor, Liquid, and Solid Phases (English Units)*, 1969, John Wiley Sons, New York, NY
13. Gifford, A. R.: "Further Development of the Heat Sponge Concept Using Water-Ammonia Mixtures," Master's Thesis, Dept. of Mechanical and Aerospace Engineering, The George Washington University, Washington, D.C., January 2005.